

## Article

# An Experimental Design Methodology to Evaluate the Key Parameters on Dispersion of Carbon Nanotubes Applied in Soil Stabilization

António Alberto S. Correia <sup>1,\*</sup> , Diogo Figueiredo <sup>2</sup> and Maria G. Rasteiro <sup>2</sup> 

<sup>1</sup> University of Coimbra, Department of Civil Engineering, CIEPQPF-Chemical Process Engineering and Forest Products Research Centre, Rua Luis Reis Santos, 3030-790 Coimbra, Portugal

<sup>2</sup> University of Coimbra, Department of Chemical Engineering, CIEPQPF-Chemical Process Engineering and Forest Products Research Centre, Rua Sílvia Lima, 3030-790 Coimbra, Portugal

\* Correspondence: aalberto@dec.uc.pt; Tel.: +351-239-797-277

**Featured Application:** Based on an experimental design strategy, two models are proposed to predict the mechanical properties of soft soil stabilized with carbon nanotubes. These models can be helpful for further developments toward the application of carbon nanotubes on soil stabilization in real situations.

**Abstract:** The incorporation of carbon nanotubes (CNTs) in the process of chemical stabilization of soft soil is only possible when they are dispersed adequately in the medium. The maximum compressive strength ( $q_{u\max}$ ) and the secant undrained Young's modulus ( $E_{u50}$ ) are usually used to characterize the behavior of soil stabilized with Portland cement. In the present study, soft soil was additivated with a CNT dispersion prepared in a surfactant solution. This information was then used to produce a model based on an experimental design strategy, which allowed us to relate  $q_{u\max}$  and  $E_{u50}$  with the CNT concentration and the surfactant hydrodynamic diameter and concentration. The Partial Least Squares (PLS) regression method was selected to perform the regression, given the significant collinearity among the input variables. The results obtained lead us to conclude that the CNT concentration is the most important factor and has a positive impact on the responses ( $q_{u\max}$  and  $E_{u50}$ ). The surfactant concentration and hydrodynamic diameter have a negative impact on the responses, but, curiously, when combined, the impact becomes positive. It means that these variables depend on each other. The results obtained show that it is possible to produce a statistical model for these parameters with good correlation coefficient ( $R^2$ ).

**Keywords:** carbon nanotubes; chemical soil stabilization; partial least squares; hydrodynamic diameter; surfactant concentration



**Citation:** Correia, A.A.S.; Figueiredo, D.; Rasteiro, M.G. An Experimental Design Methodology to Evaluate the Key Parameters on Dispersion of Carbon Nanotubes Applied in Soil Stabilization. *Appl. Sci.* **2023**, *13*, 4880. <https://doi.org/10.3390/app13084880>

Academic Editors: Mian C. Wang and Mien Jao

Received: 3 March 2023

Revised: 28 March 2023

Accepted: 10 April 2023

Published: 13 April 2023



**Copyright:** © 2023 by the authors. Licensee MDPI, Basel, Switzerland. This article is an open access article distributed under the terms and conditions of the Creative Commons Attribution (CC BY) license (<https://creativecommons.org/licenses/by/4.0/>).

## 1. Introduction

The growing socio-economic development in modern societies has led to an increase in soil requirements in terms of stability and safety. Thus, new technical solutions have been proposed to improve soils characterized by poor mechanical properties (unsuitable strength and deformability). One of the techniques to make construction possible on such soils is chemical stabilization, which has been used with success during the last decades [1–3]. However, in order to maximize feasibility, it is crucial for the development of techniques to optimize the performance of cement-stabilized soil, namely to improve its mechanical behavior.

The performance of chemically stabilized soil can be considerably improved by the incorporation of nanometric particles in the modified soil–binder matrix since they have the ability to fill the pores of the matrix at the nanometric scale, which can be reflected in a more solid and strong matrix [3–5]. However, direct application of such materials is

not possible due to the natural tendency for aggregation of these particles, which causes a loss in the beneficial effects associated with their incorporation [6–9]. Carbon nanotubes (CNTs) have unique properties, making them very attractive for application in composite materials [3,9–12]. Currently, the most widespread use of CNT nanocomposites is in electronics. These nanocomposites could be used to shield electromagnetic interference and as electrostatic-discharge components [13]. The removal of heavy metals from wastewaters [14], catalyst supporters [15,16], and chemical sensors [17,18] are other areas where CNTs are widely applied. However, as mentioned above, carbon nanotubes have a high tendency to aggregate when used in suspension, which results in a loss of its properties [19]. This problem can be solved by the addition of surfactants that promote the dispersion of the particles in the suspension or through the functionalization of CNT surface [9,12,20–24].

The mechanical behavior of soil can be improved by the mixture of chemical materials (binders with cementitious properties) with the natural soil [25–28]. The cementitious products resulting from the physico-chemical interactions originate a new composite material with a better mechanical behavior than the original soil [19,29–32]. There is the possibility to improve this behavior even more by the addition of carbon nanotubes due to their unique properties, namely a high specific surface (high capacity to interact with other particles in the surrounding environment), and extremely high yield strength and moduli of elasticity (making them an excellent reinforcing material) [3,19,33,34]. If carbon nanotubes are properly dispersed in a soil–cement matrix, they may act as a nanofiller and a nano-reinforcement agent, thereby promoting a denser and stronger stabilized matrix [3].

In order to disperse CNTs (applied in different concentrations), ultra-sounds were applied to aqueous solutions enriched with surfactants (varying in type and concentration). The quality of the CNTs' dispersion was evaluated through dynamic light scattering (DLS). Afterward, the suspensions were mixed with the binder and soil, and laboratory samples were prepared. At the end, the samples were submitted to unconfined compression strength (UCS) tests [26,35,36] in order to characterize the mechanical behavior of the new soil–binder–CNT material. The samples were compressed until failure while automatically recording the load and the vertical displacement. The unconfined compression strength ( $q_{u \max}$ ) was characterized by the maximum load recorded during the UCS test, while the stiffness ( $E_{u 50}$ ) was described by the secant undrained Young's modulus evaluated at 50% of the compression strength [26,37].

The parameters studied in this work are the type and concentration of surfactant, and the concentration of CNTs. The major goal of this work is to produce a predictive model based on experimental data, which allows the correlation of two mechanical properties ( $q_{u \max}$  and  $E_{u 50}$ ) with the parameters under study, thus supplying an easier way of selecting the best conditions to stabilize a specific soil. The Partial Least Squares (PLS) regression was chosen as the statistical methodology to reach an adequate relationship.

This paper starts with a brief description of the materials and experimental procedures used. Afterward, the statistical methodology is presented (PLS and cross-validation description). Then, two predictive models are developed to establish the relationship between the response variables ( $q_{u \max}$  and  $E_{u 50}$ ) and the three predictor variables (i.e., the parameters studied here). In the last section, the main results of this work are concisely presented and discussed.

## 2. Experimental Work

### 2.1. Materials

In this work, two surfactants were used, which differed in molecular weight and charge: Glycerox (glyceryl cocoate) and Amber 4001 (polyamide), supplied by AquaTech, La Plaine, Switzerland. Their features are described in Table 1. The surfactants were selected based on the charge of both the CNTs and cement particles in order to favor the interaction between the surfactant and particles, aiming to ensure their good dispersion, as described in [19]. Thus, since both CNTs and cement particles possess negative charge, a quasi-neutral surfactant and a cationic one were selected (see Table 1). Glycerox acts essentially through

the steric mechanism, while for Amber 4001, the predominant stabilization mechanism is based on electrostatic interactions. Additionally, these surfactants with quite different molecular weight, which affects the hydrodynamic diameter of the surfactant molecules, were selected in order to study the effect of this parameter on the stabilization process since it affects the CNT dispersion, which can have a potential influence on the spacing between particles (namely CNTs and cement), with repercussions on the mechanical behavior of the stabilized soil enriched with CNTs [34].

**Table 1.** Surfactant characteristics.

Surfactant (–)	Charge (–)	Molecular Weight (kDa)	Hydrodynamic Diameter (nm)
Glycerox	Nonionic	4265	41.95
Amber 4001	Cationic	54	5.65

While the charge was provided by the supplier, molecular weight and hydrodynamic diameter were experimentally determined using light scattering methods. Molecular weight was determined by static light scattering and hydrodynamic diameter was determined by dynamic light scattering (DLS), both in the Nanosizer ZSN from Malvern, UK.

Multiwall carbon nanotubes (MWCNTs) supplied by Nanocyl, Sambreville, Belgium, product NC7000, were used. The choice for MWCNTs was mainly due to economic factors; MWCNTs are significantly less expensive than single-wall carbon nanotubes and, so far, only MWCNTs are produced at an industrial level [34,38]. According to the supplier information, the MWCNTs have an average diameter of 9.5 nm, an average length of 1500 nm, an average specific surface of 275,000 m<sup>2</sup>/kg, and their chemical composition is pure carbon (90%) with some metal oxides (10%), as described in Table 2. MWCNTs have a negative electrical charge (–25.2 mV) as measured by electrophoretic light scattering in the Nanosizer ZSN from Malvern, UK [33]. According to Kobashi et al. [38], the MWCNTs selected for this study are classified as CNTs with low crystallinity, i.e., they exhibit a greater potential capacity to interact with the surrounding particles.

**Table 2.** MWCNT characteristics.

Average Diameter (nm)	Average Length (nm)	Carbon Purity (%)	Metal Oxides (%)	Average Specific Area (m <sup>2</sup> /kg)	Average Charge (mV)
9.5	1500	90	10	275,000	–25.2

The grain size composition of the natural soil is made of 66% of silt, 22% of sand, and 12% of clay particles. In general, it is a soft soil with low strength, low permeability, and high compressibility, and it presents a high value of water content (80.87%) and organic matter content (9.3%), which are reflected in its weak geotechnical characteristics. Table 3 summarizes the main geotechnical properties and the mineralogical and chemical compositions of the natural soft soil. More details can be seen in Figueiredo et al. [19] and in Figueiredo [33].

The binder chosen for this study was Portland cement because it is the binder material used in practice in the majority of soil stabilization cases [3]. A Portland cement type I was selected, which is a mechanical strength class of 42.5 R (CEM I 42.5 R), and its mixture with water spontaneously initiates a physico-chemical process known as hydration reaction. The binder is mostly composed of CaO (62.84%) and SiO<sub>2</sub> (19.24%) as stated in the technical data supplied by the producer (Cimpor, Coimbra, Portugal) and shown in Table 4. The cement particles are slightly negatively charged on average (zeta potential measured using electrophoretic light scattering, in the Nanosizer ZSN from Malvern, is –2.14 mV), which is in accordance with Srinivasan et al. [39].

**Table 3.** Natural soil characteristics (average values).

<b>Geotechnical Characterization</b>							
Sand (%)	Silt (%)	Clay (%)	Water Content (%)	Organic Matter Content (%)	Unit Weight (kN/m <sup>3</sup> )	Specific Gravity (-)	Porosity (%)
22	66	12	80.87	9.3	14.6	2.555	67.8
<b>Mineralogical Composition</b>							
Quartz (%)	Feldspar K + Muscovite (%)	Vermiculite (%)	Illite (%)	Kaolinite (%)	Chlorite Fe (%)		
>60–65	<25–30	4.6	2.4	1.5	1.5		
<b>Chemical Composition</b>							
CaO (%)	SiO <sub>2</sub> (%)	Al <sub>2</sub> O <sub>3</sub> (%)	Fe <sub>2</sub> O <sub>3</sub> (%)	MgO (%)	K <sub>2</sub> O (%)	pH (-)	
0.74	62.00	16.00	4.80	1.10	3.00	3.50	

**Table 4.** Portland cement characteristics (average values).

CaO (%)	SiO <sub>2</sub> (%)	Al <sub>2</sub> O <sub>3</sub> (%)	Fe <sub>2</sub> O <sub>3</sub> (%)	MgO (%)	SO <sub>3</sub> (%)	Cl <sup>-</sup> (%)	Charge (mV)
62.84	19.24	4.93	3.17	2.50	3.35	0.01	−2.14

## 2.2. Experimental Methodology

The laboratory procedure is schematically represented in Figure 1. It starts with the dispersion of the MWCNTs in the surfactant solution, following the procedure described in [19] (add the required amount of surfactant (Glycerox or Amber 4001) and apply ultrasounds (20 kHz) for 5 min to the suspension). The quality of the dispersion was indirectly evaluated by statistical models that relate the mechanical properties ( $q_{u\ max}$  and  $E_{u\ 50}$ ) of the stabilized soil with the parameters of the CNT suspension. Afterward, all materials were mixed in a mechanical mixer Hobart N50 at a rotational speed of 136 rpm. Next, laboratory samples were produced and cured for 7 days. Finally, UCS performance tests were conducted in a universal testing machine (Wykeham Farrance—Tristar 5000, UK) to demonstrate the added value of using the MWCNT dispersion in soil stabilization.

The performance tests were planned by changing the concentration of the surfactant (0, 0.5, 1, 2, and 3%), the type of surfactant (varying the hydrodynamic diameter one order of magnitude) and the MWCNT concentration (0, 0.001, and 0.01%, defined as the ratio of the weight of MWCNTs to the dry weight of Portland cement).

For each different test condition, at least two specimens were tested. A conformity criterion was adopted based on compressive strength ( $q_{u\ max}$ ): a specimen test is only accepted when the deviation from the average value is less than 15% (in the absence of standards for this type of materials, the recommendations for concrete were adopted [40]).

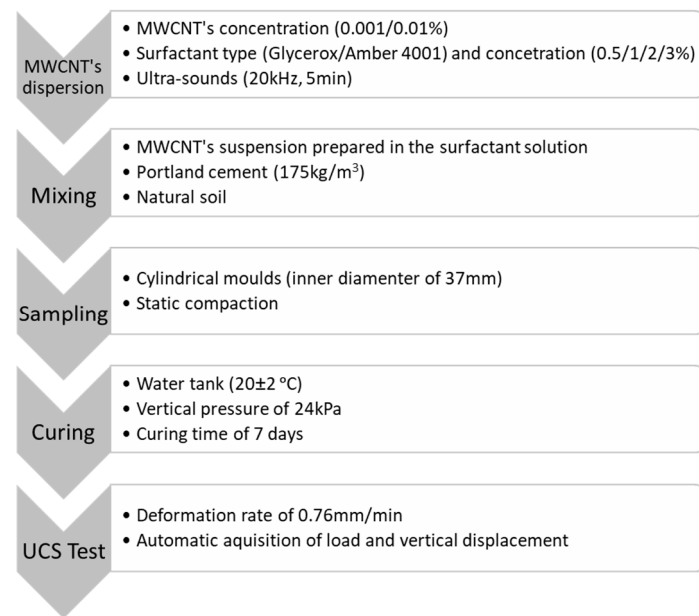


**Figure 1.** Schematic representation of the laboratory procedure.

### 3. Statistical Methods—Partial Least Squares

Statistical methods can help in identifying which variables in a system can be controlled (factors) to explain and predict the behavior of the output variables (responses).

Different strategies can be used to establish these relationships, namely Multilinear Regression (MLR) [41] and Partial Least Squares (PLS) [42]. MLR is used when the number of factors is small; the factors are not collinear; and the relationship between the factors and responses can be in some way understood a priori [43]. When any of these three conditions is not present, MLR is not an adequate strategy to establish a model relating the factors to the responses. On the other hand, PLS can be an appropriate strategy to predict the dependent variables from a large set of independent variables, which are called, in this case, predictors, even if there is a high degree of collinearity between the independent variables. PLS relates two data matrices: the predictor (input variable) matrix (X variables) and the response matrix (Y variables), making use of a linear multivariate model for that purpose [42,44].

PLS is a bilinear calibration method that calculates linear combinations of input variables that have a maximum covariance with the response. These linear combinations (latent variables) are found sequentially. Each combination results from the progressive analysis of a different part of the space until prediction ability stops improving, based on the analysis of the value of the predicted determination coefficient ( $R^2$  (pred)).

Minitab (version 17.1.0) was the software used to apply the PLS method to the data set in the present study. Minitab uses the Nonlinear Iterative Partial Least Squares (NIPALS) algorithm developed by Herman Wold [45–48]. This algorithm reduces the number of predictors using a technique similar to principal components analysis by extracting a set of components that describes the maximum correlation between the predictors and the response variables. If the predictors are highly correlated, then the number of components in the model might be much less than the number of predictors. Minitab then performs least squares regression on the uncorrelated components. Additionally, cross-validation is often used to select the components that maximize the model's predictive ability [47,48].

To validate the model, the best approach is to use an independent data set or “test set” and to check the predictive ability of the model based on the results obtained for the independent data set (external validation). However, when the data set collected is small, it is sometimes impossible, in order to validate the model, to guarantee access to an independent test set. In that case, the alternative is to perform what is called a cross-

validation by creating “test sets” within the “training data set”, i.e., the data set used to create the model itself (internal validation) [49].

In the case of internal validation, the training data set is divided into blocks; one block is left aside in each run, and a new model is obtained with the remaining blocks, which is used to estimate the response of the removed blocks. The cross-validation prediction errors are calculated for this new situation, and this process is repeated successively, each time removing a new block while the previously removed one is integrated again in the training data set. The overall cross-validation error will be estimated once this process is completed [48–50]. At the end of the cross-validation process, it is also possible to determine the model dimension, i.e., the number of PLS components (latent variables) the model should have.

In this study, this last methodology was used due to the lack of additional experimental data to be used as an independent test set.

#### 4. Results and Discussion

As shown by Figueiredo (2014), the mechanical properties ( $q_{u\ max}$  and  $E_{u\ 50}$ ) of a soft soil chemically stabilized with Portland cement can be significantly improved by the addition of CNTs when they are dispersed adequately in the medium [33]. Thus, the improvement is somehow related with the surfactants’ characteristics and CNT concentration.

In the present work, the mechanical properties,  $q_{u\ max}$  and  $E_{u\ 50}$ , were studied as the response variables in two different tests. In both tests, three predictor variables were considered: surfactant concentration ( $x_1$ ), surfactant hydrodynamic diameter ( $x_2$ ), and CNT concentration ( $x_3$ ).

The main objective of this study was to identify the most important variables for the relationship between the response and the predictor variables and to find the combination of factors that better described the  $q_{u\ max}$  and  $E_{u\ 50}$ . The PLS methodology was used for this purpose. In every test, each set of conditions (surfactant type and concentration and CNT concentration) was repeated at least twice. However, in the PLS regression modeling, each test was considered individually, i.e., the values in the matrix were not the average values of the repetitions, but the individual values for each sample.

##### 4.1. Case 1: $q_{u\ max}$

A full quadratic model was estimated by PLS regression after expanding the original data set with the quadratic and cross-product terms of the quadratic expansion. All variables were considered as continuous variables.

Figure 2 represents the evolution of the model’s coefficients of determination versus the number of components of the PLS model, and Figure 3 corresponds to the predicted response versus the actual response in the leave-one-out cross-validation (where the cross-validation blocks are formed by a single observation).

The vertical line in Figure 2 shows that the optimum model has five components and can explain 70% of the model response. The response plot (Figure 3) indicates that the model predicts the removed observations quite well. Although there are differences between the fitted and cross-validated fitted models, none are severe enough to indicate an extreme leverage point.

The ANOVA test of the model for  $q_{u\ max}$  with five components is presented in Table 5, which shows the degree of freedom (DF), the sum of squares (SS), the mean square (MS), and the F- and P-tests. As the  $p$ -value is under 0.05, the model is significant [51].

Table 5 also shows the variance of the indicators (X variance), the error (Er), the square error ( $R^2$ ), the prediction sum squares (PRESS), and the predicted determination coefficient ( $R^2$  (pred)). The model with five components has a reasonably high  $R^2$  of 78% and  $R^2$ (pred) of 70% (Table 5), providing good indicators for its fitting ability and predictive accuracy. The regression coefficients for the  $q_{u\ max}$  model were used with the predictors to calculate the fitted value of the response variables, and the results are listed in Table 6.

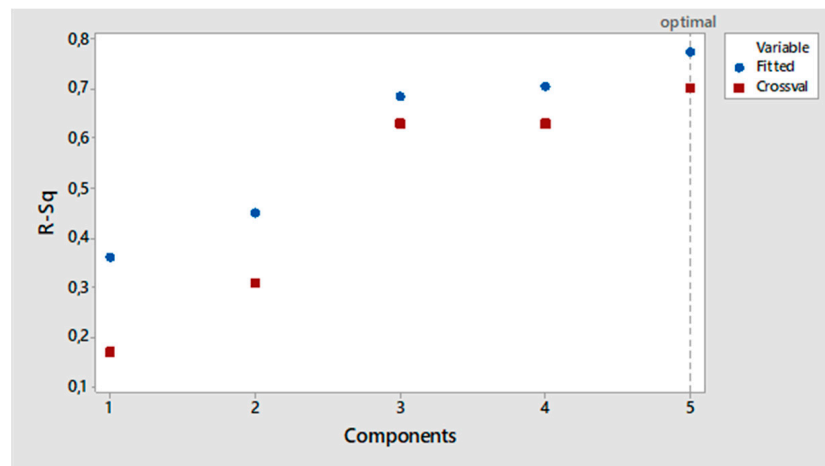


Figure 2. PLS model selection plot— $q_{u \max}$ .

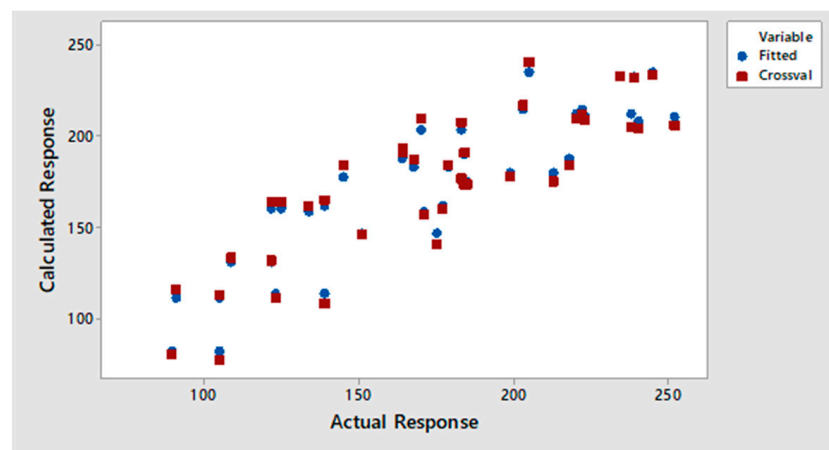


Figure 3. PLS response plot (5 components)— $q_{u \max}$ .

Table 5. Summary of the performance statistics for the PLS model— $q_{u \max}$ .

ANOVA Test					
Source	DF	SS	MS	F-test	P-test
Regression	5	65,501.9	13,100.4	24.25	0.000
Residual Error	35	18,905.7	540.2		
Total	40	84,407.6			

Performance Statistics for the PLS Model					
Components	X Variance	Er	R <sup>2</sup>	PRESS	R <sup>2</sup> (pred)
1	0.27653	53,943.3	0.360919	70,208.9	0.168216
2	0.58601	46,419.1	0.450060	58,481.8	0.307150
3	0.67210	26,476.7	0.686324	31,339	0.628718
4	0.99928	24,830.4	0.705828	31,357.6	0.628498
5	1.00000	18,905.7	0.776019	25,195.1	0.701507

In a PLS regression, standardized coefficients identify the importance of each predictor in the model and correspond to the standardized X variables and standardized Y variables. The coefficient matrix (dimension p.r, where p = number of predictors and r = number of responses) is calculated from the x-weights and x-loadings [50]. Standardization of the variables can be conducted in different ways. In this study, for the normalization of the variables, the procedure of subtracting the mean and dividing by the standard deviation

was used. In this way, multicollinearity resulting from the interaction terms can be minimized [50]. From the magnitude and sign of the standardized coefficients (Table 6), it can be seen that the CNT concentration ( $x_3$ ) and its quadratic relation ( $x_3 \cdot x_3$ ) are the most important factors influencing the response ( $q_{u \max}$ ). While  $x_3$  has a positive effect on  $q_{u \max}$ ,  $x_3 \cdot x_3$  has a negative impact. It means that the CNT concentration has a non-linear effect in the response, i.e., there is an optimum value of CNT concentration that maximizes the response. Indeed, as the concentration of MWCNTs increases, the probability of agglomeration increases, resulting in a loss of their beneficial properties. On the other hand, the surfactant concentration ( $x_1$ ) and surfactant hydrodynamic diameter ( $x_2$ ) have a negative impact on  $q_{u \max}$ , but, curiously, when combined ( $x_1 \cdot x_2$ ) the impact becomes positive. It means that these variables depend on each other. Indeed, an increase in the surfactant concentration or surfactant hydrodynamic diameter promotes larger particles' spacing (especially regarding cement particles), resulting in a less strong and stiff stabilized matrix. However, when both effects are combined, the impact on unconfined compression strength ( $q_{u \max}$ ) becomes positive, meaning that these two variables (surfactant concentration and surfactant hydrodynamic diameter) depend on each other. In fact, if a surfactant has a higher hydrodynamic diameter, less molecules will be necessary to cover the surface of the CNTs, and, thus, a lower concentration of the surfactant will be required to guarantee a good dispersion of the CNTs. Thus, the two variables are correlated, as expected.

**Table 6.** Regression coefficients for the  $q_{u \max}$  model.

Component	$q_{u \max}$ (kPa)	$q_{u \max}$ Standardized
Intercept	243	0
1- $x_1$	-60	-1.2
2- $x_2$	-3	-1.0
3- $x_3$	34,203	3.3
4- $x_1 \cdot x_2$	2	1.2
5- $x_3 \cdot x_3$	-3,131,470	-3.2

The PLS residual versus leverage is useful to understand the distribution of the observations. Figure 4 confirms the significance of the data set. The leverage of an observation measures its ability to move the regression model as a whole by simply moving in the y-direction. The leverage always takes values between zero and one. A point with zero leverage has no effect on the regression model. If a point has a leverage equal to one, the line must follow the point perfectly. As all points are inside the defined limits and no outlier is present, the data set is significant.

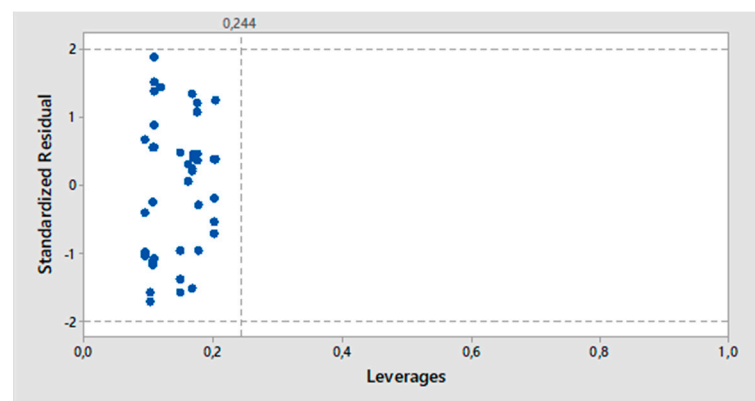


**Figure 4.** PLS residual vs. leverage plot for the  $q_{u \max}$  model.

The surface plot shows the behavior of  $q_{u \max}$  with  $x_1$  and  $x_3$  (Figure 5) and  $x_2$  and  $x_3$  (Figure 6). As expected, it is a non-linear relation.  $q_{u \max}$  increases with  $x_2$  (higher surfactant

hydrodynamic diameter leads to higher  $q_{u\max}$ ) and shows an optimum regarding  $x_1$  (surfactant concentration) and  $x_3$  (CNT concentration).

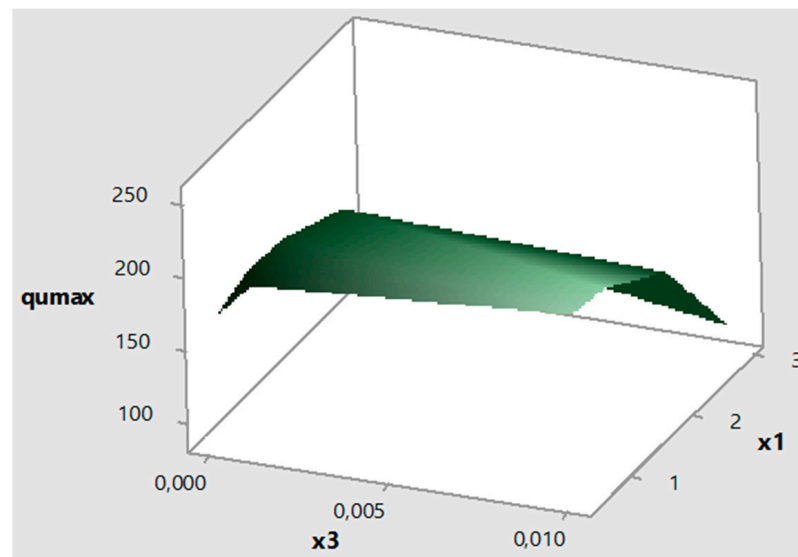


**Figure 5.** Surface plot of  $q_{u\max}$  vs.  $x_1$  and  $x_3$ .

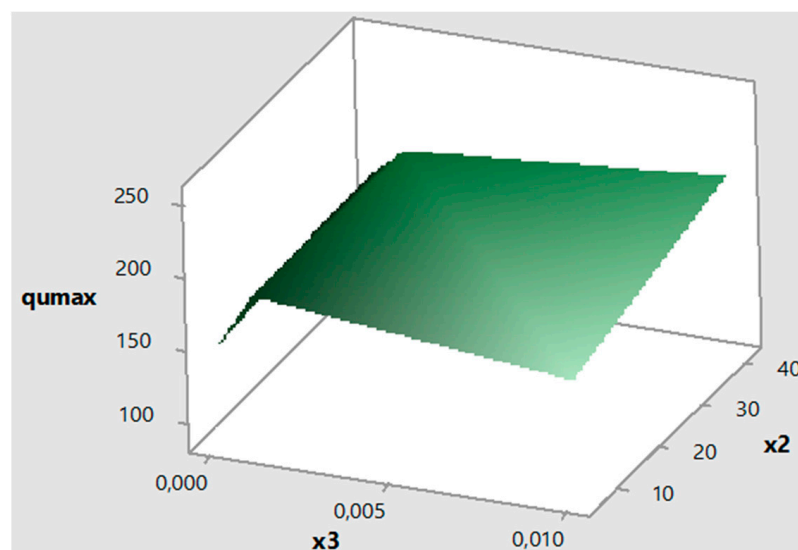


**Figure 6.** Surface plot of  $q_{u\max}$  vs.  $x_2$  and  $x_3$ .

In order to better understand the structure of the composite material, Figure 7 shows a scanning electron microscope (SEM) image of a stabilized soil sample additivated with MWCNTs dispersed in an aqueous solution of Amber 4001. Three kinds of materials can be identified in the SEM image: the needle-shaped lattice materials are calcium silicate associated with the Portland cement reactions with water, the materials in the form of irregular polyhedrons are soil particles, while the long and narrow particles are the MWCNTs. As can be seen from Figure 7, the MWCNTs are adequately dispersed in the matrix due to the effect of the surfactant, thus ensuring that the beneficial properties associated with the presence of the MWCNTs are not lost. The low crystallinity of the MWCNTs [38] ensures good interaction with surrounding particles, in particular with Portland cement particles. Thus, these results suggest that the MWCNTs seem to give some continuity to the calcium silicates produced by the Portland cement, allowing the establishment of denser

cementitious bonds, i.e., the CNTs seem to act as a nanofiller and a nano-reinforcement agent, promoting the construction of a denser and more resistant structure.

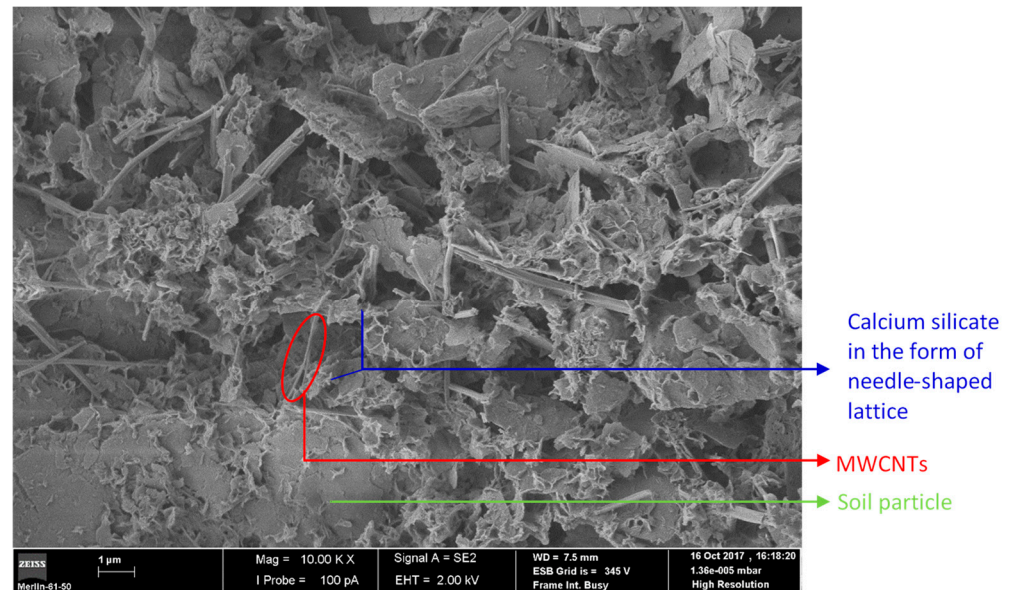


**Figure 7.** SEM image of a chemically stabilized soil sample additivated with MWCNTs (0.01%) dispersed in a solution of Amber 4001 (3%) for 7 curing days.

#### 4.2. Case 2: $E_{u50}$

A similar study was performed for  $E_{u50}$ . A full quadratic model was estimated by PLS regression after expanding the original data set with the quadratic and cross-product terms of the quadratic expansion. All variables were considered as continuous variables. The detailed explanations given in the previous section will not be repeated again.

The model selection plot (Figure 8) sets the optimal model with five components, which can predict 89% of the model response. The response plot (Figure 9) shows that the model predicts quite well the predicted response versus the actual response in the leave-one-out cross-validation.

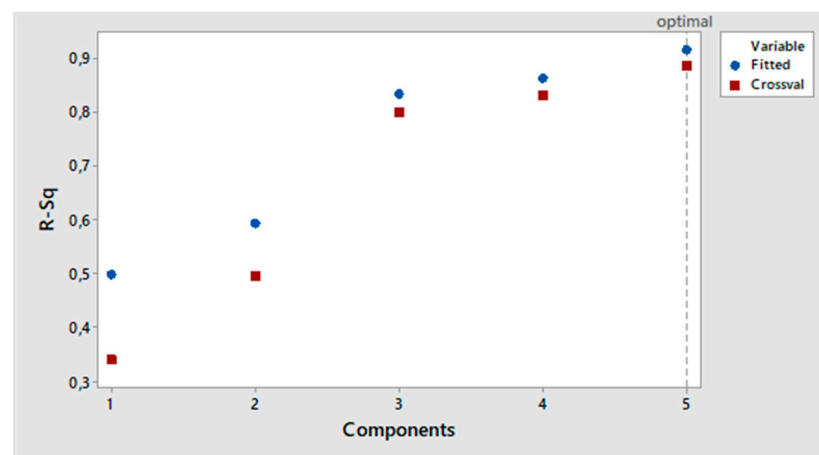


**Figure 8.** PLS model selection plot— $E_{u50}$ .

The ANOVA test for the PLS model with five components is presented in Table 7. Once again, as the  $p$ -value is under 0.05, the model is significant [51]. Table 7 also shows the performance statistics for the PLS model. Statistically, the model with five components

has a quite high  $R^2$  of 92% and  $R^2$  (pred) of 89% (Table 7), which are good indicators of its fitting ability and predictive accuracy.

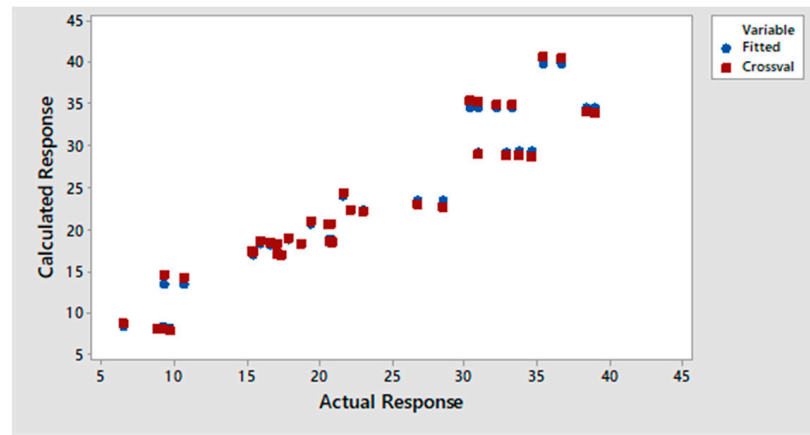


Figure 9. PLS response plot (5 components)— $E_{u 50}$ .

Table 7. Summary of the performance statistics for the PLS model— $E_{u 50}$ .

ANOVA Test					
Source	DF	SS	MS	F-test	P-test
Regression	5	2906.39	581.278	71.46	0.000
Residual Error	33	268.42	8.134		
Total	38	3174.81			

Performance Statistics for the PLS Model					
Components	X Variance	Er	$R^2$	PRESS	$R^2$ (pred)
1	0.28485	1596.57	0.497112	2098.69	0.338954
2	0.60152	1292.49	0.592890	1607.12	0.493788
3	0.69374	531.93	0.832454	633.92	0.800329
4	0.99941	433.51	0.863453	539.30	0.830132
5	1.00000	268.42	0.915454	362.65	0.885773

The analysis of the standard coefficients of  $E_{u 50}$  (Table 8) leads to similar conclusions as for  $q_{u \max}$ . The MWCNT concentration ( $x_3$ ) and its quadratic relation ( $x_3.x_3$ ) are the most important factors influencing the response ( $E_{u 50}$ ). While  $x_3$  has a positive effect on  $E_{u 50}$ ,  $x_3.x_3$  has a negative impact. It means that the CNT concentration has a non-linear behavior, i.e., there is an optimum value of CNT concentration that maximizes the response. As stated previously, the probability of agglomeration increases with the MWCNT concentration, resulting in a loss of MWCNT beneficial properties. On the other hand, the surfactant concentration ( $x_1$ ) and surfactant hydrodynamic diameter ( $x_2$ ) have a negative impact on  $E_{u 50}$ , but, once again, when combined ( $x_1.x_2$ ), the impact becomes positive, meaning that these variables depend on each other. Standardization was conducted in a similar way as for  $q_{u \max}$ . As it was previously discussed, an increase in the surfactant concentration or surfactant hydrodynamic diameter promotes particles' spacing (especially regarding cement particles), resulting in a less strong and stiff stabilized matrix. Again, when both effects are combined, the impact on  $E_{u 50}$ , the undrained Young's modulus, becomes positive, meaning that these two variables (surfactant concentration and surfactant hydrodynamic diameter) depend on each other, following what was observed previously for  $q_{u \max}$ .

**Table 8.** Regression coefficients for the  $E_{u50}$  model.

Component	$E_{u50}$ (MPa)	$E_{u50}$ Standardized
Intercept	44	0
1-x1	-13	-1.2
2-x2	-1	-1.3
3-x3	5857	3.0
4-x1x2	0	0.9
5-x3x3	-58,4973	-3.1

The PLS residual vs. leverage plot (Figure 10) shows at least two points in the border of leverage; thus, they can be considered as possible outliers, but the result continues to be significant.

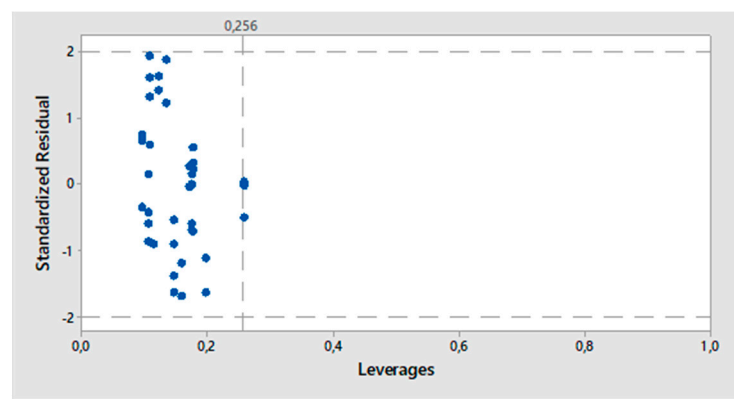


**Figure 10.** PLS residual vs. leverage plot— $E_{u50}$ .

The behavior of  $E_{u50}$  as a function of  $x_1$  and  $x_3$  and a function of  $x_2$  and  $x_3$  is represented in Figures 11 and 12, respectively. As expected, again, a non-linear relation is observed. The model presents an optimum for  $x_3$  (CNT concentration) and  $x_1$  (surfactant concentration), while  $x_2$  (surfactant hydrodynamic diameter—related to the type of surfactant) influences  $E_{u50}$  only slightly.

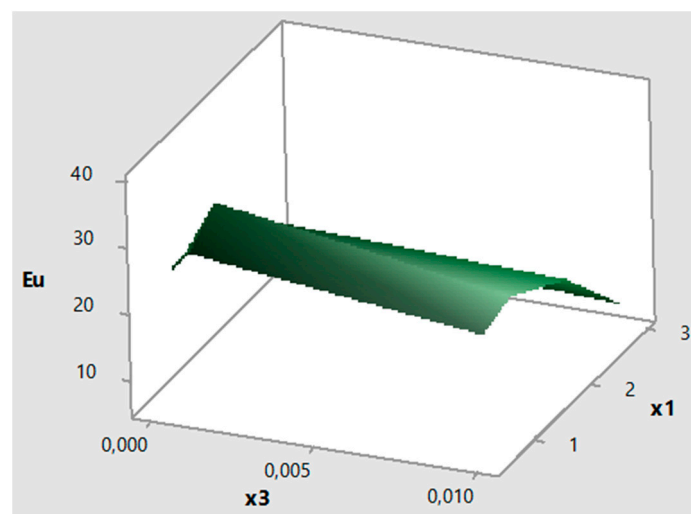


**Figure 11.** Surface plot of  $E_{u50}$  vs.  $x_1$  and  $x_3$ .

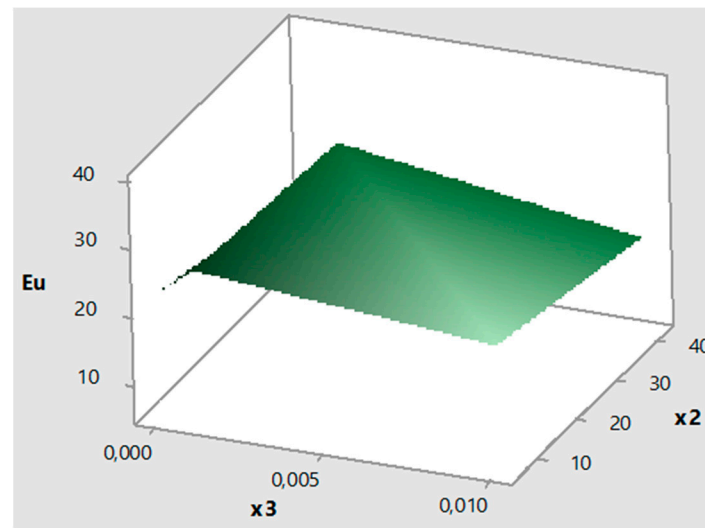


**Figure 12.** Surface plot of  $E_{u\ 50}$  vs.  $x_2$  and  $x_3$ .

## 5. Conclusions

Cementitious composites reinforced with MWCNTs were developed and applied to soft soil to improve its mechanical properties. Two surfactants with different hydrodynamic diameters were used to disperse the MWCNTs in water. A preliminary analysis of the results obtained showed that the mechanical properties of the soft soil chemically improved with the addition of MWCNTs is mainly related to three variables: the concentration and the hydrodynamic diameter of the surfactant and the MWCNT concentration. The improvement in the mechanical properties in relation with these three variables was assessed by determining  $q_{u\ max}$  and  $E_{u\ 50}$ .

A PLS methodology was used to identify the influence of each variable on  $q_{u\ max}$  and  $E_{u\ 50}$ , and two models were constructed, namely a model for  $q_{u\ max}$  and a model for  $E_{u\ 50}$ .

In both cases, the optimum model was composed of five components, and the model of  $q_{u\ max}$  can explain 70% of the model response while the model for  $E_{u\ 50}$  is able to explain 89% of the model response. However, the conclusions regarding the influence of the variables on the response parameters are very similar for the two parameters. The MWCNT concentration is the most important factor and has a positive impact on the response ( $q_{u\ max}$  and  $E_{u\ 50}$ ). However, it was observed that the probability of agglomeration increases with the MWCNT concentration, meaning that there is an optimum value of MWCNT concentration that maximizes the response. The surfactant concentration and surfactant hydrodynamic diameter have a negative impact on the response, but, curiously, when combined, the impact becomes positive. It means that these variables depend on each other. Indeed, the MWCNTs are directly responsible for improving the mechanical performance of the stabilized soil, while the surfactant properties ensure a better performance of the MWCNTs.

Considering the results obtained, it is possible to propose two models for both  $q_{u\ max}$  and  $E_{u\ 50}$  when MWCNTs are added to the binder for soil stabilization purposes. These models can be helpful for further developments toward the application of carbon nanotubes on soil stabilization in real situations.

**Author Contributions:** A.A.S.C. participated in the conceptualization, validation, supervision, writing and editing of the manuscript; D.F. conducted the experimental investigation and prepared the first draft of the manuscript; M.G.R. was responsible for the conceptualization and participated in the validation and supervision of the research and in the review and editing of the manuscript. All authors have read and agreed to the published version of the manuscript.

**Funding:** This research was funded by the Strategic Research Centre (CIEPQPF) Project UIDB00102/2020 and by the research project PTDC/ECI-CON/28382/2017, both funded by the FCT (Fundação para a Ciência e Tecnologia), Portugal.

**Institutional Review Board Statement:** Not applicable.

**Informed Consent Statement:** Not applicable.

**Data Availability Statement:** Some or all data, models, or code generated or used during the study are available from the corresponding author upon reasonable request.

**Acknowledgments:** The authors acknowledge AquaTech, Switzerland, and Cimpor, Portugal, for supplying, respectively, the surfactants and the binders used in the work.

**Conflicts of Interest:** The authors declare no conflict of interest.

## References

1. Mitchell, J.K. Practical problems from surprising soil behavior. *J. Geotech. Eng.* **1986**, *112*, 259–289.
2. Bergado, D.T.; Anderson, L.R.; Miura, N.; Balasubramaniam, A.S. *Soft Ground Improvement in Lowland and Other Environments*; ASCE Press: New York, NY, USA, 1996.
3. Correia, A.A.S.; Casaleiro, P.D.F.; Rasteiro, M.G. Applying multiwall carbon nanotubes for soil stabilization. *Procedia Eng. Spec. Issue New Paradig. Part. Sci. Technol.* **2015**, *102*, 1766–1775. [[CrossRef](#)]
4. Choudhary, V.; Gupta, A. *Polymer/Carbon Nanotube Nanocomposites. Carbon Nanotubes—Polymer Nanocomposites*; Yellampalli, S., Ed.; InTech: London, UK, 2011; ISBN 978-953-307-498-6.
5. Konsta-Gdoutos, M.S.; Metaxa, Z.S.; Shah, S.P. Highly dispersed carbon nanotube reinforced cement-based materials. *Cem. Concr. Res.* **2010**, *40*, 1052–1059. [[CrossRef](#)]
6. Singh, V.; Joung, D.; Zhai, L.; Das, S.; Khondaker, S.; Seal, S. Graphene based materials: Past, present and future. *Prog. Mater. Sci.* **2011**, *56*, 1178–1271. [[CrossRef](#)]
7. Kuila, T.; Bose, S.; Mishra, A.; Khanra, P.; Kim, N.; Lee, J.H. Chemical functionalization of graphene and its applications. *Prog. Mater. Sci.* **2012**, *57*, 1061–1105. [[CrossRef](#)]
8. Nasibulin, A.G.; Koltsova, T.; Nasibulina, L.I.; Anoshkin, I.V.; Semench, A.; Tolochko, O.V.; Kauppinen, E.I. A novel approach to composite preparation by direct synthesis of carbon nanomaterial on matrix or filler particles. *Acta Mater.* **2013**, *61*, 1862–1871. [[CrossRef](#)]
9. Gao, Y.; Jing, H.; Du, M.; Chen, W. Dispersion of Multi-Walled Carbon Nanotubes Stabilized by Humic Acid in Sustainable Cement Composites. *Nanomaterials* **2018**, *8*, 858. [[CrossRef](#)] [[PubMed](#)]
10. Saleem, H.; Zaidi, S.J. Recent Developments in the Application of Nanomaterials in Agroecosystems. *Nanomaterials* **2020**, *10*, 2411. [[CrossRef](#)]
11. Liu, G.; Zhang, C.; Zhao, M.; Guo, W.; Luo, Q. Comparison of Nanomaterials with Other Unconventional Materials Used as Additives for Soil Improvement in the Context of Sustainable Development: A Review. *Nanomaterials* **2021**, *11*, 15. [[CrossRef](#)]
12. Metaxa, Z.S.; Boutsioukou, S.; Amenta, M.; Favvas, E.P.; Kourkoulis, S.K.; Alexopoulos, N.D. Dispersion of Multi-Walled Carbon Nanotubes into White Cement Mortars: The Effect of Concentration and Surfactants. *Nanomaterials* **2022**, *12*, 1031. [[CrossRef](#)]
13. Choudhary, V.; Dhawan, S.K.; Saini, P. Polymer based nanocomposites for electromagnetic interference (EMI) shielding. *Polym. Adv. Technol.* **2010**, *21*, 67–100.
14. Mubarak, N.M.; Sahu, J.N.; Abdullah, E.C.; Jayakumar, N.S. Removal of heavy metals from wastewater using carbon nanotubes. *Sep. Purif. Rev.* **2014**, *43*, 311–338. [[CrossRef](#)]
15. Planeix, J.M.; Coustel, N.; Coq, B.; Brotons, V.; Kumbhar, P.S.; Dutartre, R.; Geneste, P.; Bernier, P.; Ajayan, P.M. Application of carbon nanotubes as supports in heterogeneous catalysis. *J. Am. Chem. Soc.* **1994**, *116*, 7935–7936. [[CrossRef](#)]
16. Che, G.; Lakshmi, B.B.; Fisher, E.R.; Martin, C.R. Carbon nanotubule membranes for electrochemical energy storage and production. *Nature* **1998**, *393*, 346–349. [[CrossRef](#)]
17. Kong, J.; Franklin, N.R.; Zhou, C.; Chapline, M.G.; Peng, S.; Cho, K.; Dai, H. Nanotube molecular wires as chemical sensors. *Science* **2000**, *287*, 622–625. [[CrossRef](#)]
18. Collins, P.G.; Bradley, K.; Ishigami, M.; Zettl, A. Extreme oxygen sensitivity of electronic properties of carbon nanotubes. *Science* **2000**, *287*, 1801–1804. [[CrossRef](#)]
19. Figueiredo, D.T.R.; Correia, A.A.S.; Hunkeler, D.; Rasteiro, M.G.B.V. Surfactants for dispersion of carbon nanotubes applied in soil stabilization. *Colloids Surf. A Physicochem. Eng. Asp.* **2015**, *480*, 405–412. [[CrossRef](#)]
20. Vaisman, L.; Wagner, H.D.; Marom, G. The role of surfactants in dispersion of carbon nanotubes. *Adv. Colloid Interface Sci.* **2006**, *128–130*, 37–46. [[CrossRef](#)]
21. Xie, X.L.; Mai, Y.W.; Zhou, X.P. Dispersion and alignment of carbon nanotubes in polymer matrix: A review. *Mater. Sci. Eng. Rep.* **2005**, *49*, 89–112. [[CrossRef](#)]
22. Correia, A.A.S.; Matos, M.P.S.R.; Gomes, A.R.; Rasteiro, M.G. Immobilization of Heavy Metals in Contaminated Soils—Performance Assessment in Conditions Similar to a Real Scenario. *Appl. Sci.* **2020**, *10*, 7950. [[CrossRef](#)]
23. Oliveira, A.R.; Correia, A.A.S.; Rasteiro, M.G. Heavy Metals Removal from Aqueous Solutions by Multiwall Carbon Nanotubes: Effect of MWCNTs Dispersion. *Nanomaterials* **2021**, *11*, 2082. [[CrossRef](#)] [[PubMed](#)]
24. Batakliov, T.; Ivanov, E.; Angelov, V.; Spinelli, G.; Kotsilkova, R. Advanced Nanomechanical Characterization of Biopolymer Films Containing GNPs and MWCNTs in Hybrid Composite Structure. *Nanomaterials* **2022**, *12*, 709. [[CrossRef](#)] [[PubMed](#)]

25. Mitchell, J.K. Soil improvement—State of the Art Report. In Proceedings of the 10th International Conference on Soil Mechanics and Foundation Engineering, Stockholm, Sweden, 15–19 June 1981; Volume 4, pp. 509–565.
26. Kitazume, M.; Terashi, M. *The Deep Mixing Method*; CRC Press: London, UK, 2013.
27. Correia, A.A.S.; Venda Oliveira, P.J.; Lemos, L.J.L. Prediction of the unconfined compressive strength in soft soil chemically stabilized. In Proceedings of the 18th International Conference on Soil Mechanics and Geotechnical Engineering: Challenges and Innovations in Geotechnics, ICSMGE 2013, Paris, France, 2–6 September 2013; pp. 2457–2460.
28. Correia, A.A.S.; Venda Oliveira, P.J.; Luis, J.; Lemos, L. Strength assessment of chemically stabilised soft soils. *Proc. Inst. Civ. Eng.—Geotech. Eng.* **2019**, *172*, 218–227. [[CrossRef](#)]
29. Porbaha, A. State of the art in deep mixing technology: Part I. Basic concepts and overview. *Ground Improv.* **1998**, *2*, 81–92. [[CrossRef](#)]
30. Horpibulsuk, S. Analysis and Assessment of Engineering Behavior of Cement Stabilized Clays. Ph.D. Dissertation, Saga University, Saga, Japan, 2001.
31. Correia, A.A.S. Applicability of Deep Mixing Technique to the Soft Soil of Baixo Mondego. Ph.D. Thesis, Department of Civil Engineering of FCTUC, University of Coimbra, Coimbra, Portugal, 2011. (In Portuguese).
32. Consoli, N.C.; Rosa, A.D.; Corte, M.B.; Lopes, L.; Consoli, B.S. Porosity-Cement Ratio Controlling Strength of Artificially Cemented Clays. *J. Mater. Civ. Eng.* **2011**, *23*, 1249–1254. [[CrossRef](#)]
33. Figueiredo, D.T.R. Characterization of Carbon Nanotubes dispersions for application in soil stabilization. Master's Thesis, Department of Chemical Engineering of FCTUC, University of Coimbra, Coimbra, Portugal, 2014.
34. Correia, A.A.S.; Casaleiro, P.D.F.; Figueiredo, D.T.R.; Moura, M.S.M.R.; Rasteiro, M.G. Key-Parameters in Chemical Stabilization of Soils with Multiwall Carbon Nanotubes. *Appl. Sci.* **2021**, *11*, 8754. [[CrossRef](#)]
35. BS 1377-7; Methods of Test for Soils for Civil Engineering Purposes—Part 7: Shear Strength Tests (Total Stress). British Standards Institution: London, UK, 1990.
36. ASTM D 2166; Standard Test Method for Unconfined Compressive Strength of Cohesive Soil. American Society for Testing and Materials: West Conshohocken, PA, USA, 2000.
37. Lorenzo, G.A.; Bergado, D.T. Fundamental characteristics of cement-admixed clay in deep mixing. *J. Mater. Civ. Eng.* **2006**, *18*, 161–174. [[CrossRef](#)]
38. Kobashi, K.; Ata, S.; Yamada, T.; Futaba, D.N.; Okazaki, T.; Hata, K. Classification of Commercialized Carbon Nanotubes into Three General Categories as a Guide for Applications. *ACS Appl. Nano Mater.* **2019**, *2*, 4043–4047. [[CrossRef](#)]
39. Srinivasan, S.; Barbhuiya, S.A.; Charan, D.; Pandey, S.P. Characterising cement—superplasticiser interaction using zeta potential measurements. *Constr. Build. Mater.* **2010**, *24*, 2517–2521. [[CrossRef](#)]
40. EN 206-1; Concrete. Specification, Performance, Production and Conformity. European Committee for Standardization: Brussels, Belgium, 2000.
41. Field, A. *Discovering Statistics Using SPSS*, 3rd ed.; Sage Publications: London, UK, 2009.
42. Wold, S.; Sjostrom, M.; Eriksson, L.T. PLS-regression: A basic tool of chemometrics. *Chemom. Intell. Lab. Syst.* **2001**, *58*, 109–130. [[CrossRef](#)]
43. Geladi, P.; Kowalski, B.R. Partial least-squares regression: A tutorial. *Anal. Chim. Acta* **1986**, *185*, 1–17. [[CrossRef](#)]
44. Pinheiro, L.; Ferreira, P.; Garcia, F.; Reis, M.; Pereira, A.; Wandrey, C.; Ahmadlooc, H.; Amaral, J.; Hunkeler, D.; Rasteiro, M. An experimental design methodology to evaluate the importance of different parameters on flocculation by polyelectrolytes. *Powder Technol.* **2013**, *238*, 2–13. [[CrossRef](#)]
45. Wold, H. Nonlinear Iterative Partial Least Squares (NIPALS) Modeling: Some Current Developments. In *Multivariate Analysis II, Proceedings of the International Symposium on Multivariate Analysis, Wright State University, Dayton, OH, USA, 19–24 June 1972*; Krishnaiah, P.R., Ed.; Academic Press: New York, NY, USA, 1973; pp. 383–407.
46. Wold, H. Soft modelling by latent variables: The non-linear iterative partial least squares (NIPALS) approach. In *Perspectives in Probability and Statistics: Papers, in Honour of M.S. Bartlett on the Occasion of His Sixty-Fifth Birthday*; Gani, J., Ed.; Applied Probability Trust, Academic: London, UK, 1975; pp. 117–142.
47. Tenenhaus, M.; Vinzi, V.E.; Chatelin, Y.-M.; Lauro, C. PLS path modeling. *Comput. Stat. Data Anal.* **2005**, *48*, 159–205. [[CrossRef](#)]
48. Minitab. What Is Partial Least Squares Regression. 2016. Available online: <http://support.minitab.com/en-us/minitab/17/topic-library/modeling-statistics/regression-and-correlation/partial-least-squares-regression/> (accessed on 27 April 2016).
49. Krstajic, D.; Buturovic, L.J.; Leahy, D.E.; Thomas, S. Cross-validation pitfalls when selecting and assessing regression and classification models. *J. Cheminformatics* **2014**, *6*, 10. [[CrossRef](#)] [[PubMed](#)]
50. Minitab. What Are the Coefficients and Standardized Coefficients in Pls Regression. 2016. Available online: <http://support.minitab.com/en-us/minitab/17/topic-library/modeling-statistics/regression-and-correlation/partial-least-squares-regression/> (accessed on 14 July 2016).
51. Montgomery, D.C.; Runger, G.C. *Applied Statistics and Probability for Engineers*, 6th ed.; Wiley: Hoboken, NJ, USA, 2014; ISBN 13 9781118539712.

**Disclaimer/Publisher's Note:** The statements, opinions and data contained in all publications are solely those of the individual author(s) and contributor(s) and not of MDPI and/or the editor(s). MDPI and/or the editor(s) disclaim responsibility for any injury to people or property resulting from any ideas, methods, instructions or products referred to in the content.